Journal of Alloys and Compounds, 191 (1993) 121–126
JALCOM 482

Tetracalcium gadolinium oxoborate ($Ca_4GdO(BO_3)_3$) as a new host lattice for luminescent materials

G. J. Dirksen and G. Blasse
Debye Research Institute, Solid State Chemistry Department, Utrecht University, P.O. Box 80.000, NL-3508 TA Utrecht (Netherlands)

(Received August 15, 1992)

Abstract

The luminescence of several trivalent ions (Gd^{3+}, Dy^{3+}, Tb^{3+}, Eu^{3+}, Ce^{3+} and Bi^{3+}) in $Ca_4GdO(BO_3)_3$ is reported. Many of these show high luminescence efficiency. Under 254 nm excitation Tb^{3+} and Eu^{3+} show a high light output. In this host lattice rapid energy migration through linear Gd^{3+} chains occurs. The O(1) ions in the host lattice which are not bonded to boron shift the energy levels of the luminescent ions to relatively low values owing to the high covalency. The Ce^{3+} ion does not luminesce in this host. This is ascribed to photoionization. The luminescence properties of activated $Ca_4Gd(BO_3)_3$ are more similar to those of the activated oxides than to those of other activated borates. This is explained on comparison of the crystal structures.

1. Introduction

Recently Norrestam *et al.* [1] described a new class of lanthanide compounds with the composition $Ca_4LnO(BO_3)_3$ (Ln≡La, Nd, Sm, Gd, Y, Er). The crystal structure consists of BO_3 triangles and one oxygen ion, O(1), which has no bond to boron. We have shown before that such an oxygen ion drastically influences the luminescence properties of ions bound to it by studying the host lattice $SrLa_2OBeO_4$ [2].

The Ln^{3+} ion in $Ca_4LnO(BO_3)_3$ is in a distorted octahedral coordination. Four oxygen ions belong to borate groups (Sm–O distances in $Ca_4SmO(BO_3)_3$ vary between 2.375 and 2.459 Å [1]) and the other two are O(1) (distances 2.254 and 2.265 Å in the case of Ln≡Sm [1]). It seemed interesting, therefore, to study the luminescence of trivalent ions on the Ln site. This site has site symmetry C_s, whereas the space group is *Cm*.

Another interesting aspect of this structure is the fact that the Ln^{3+} ions form linear chains along the *c* axis. The shortest Ln–Ln distance in this chain is equal to the *c* parameter (3.557 Å for Ln≡Gd [1]). This suggests rapid one-dimensional energy migration along the *c* axis [3], the more so because the distance between nearest chains is more than twice this Ln–Ln distance.

As host lattice we selected $Ca_4GdO(BO_3)_3$. This lattice allows visible emission from other lanthanide ions. Also, energy migration among the Gd^{3+} ions is expected to be observed. Actually, our results show that this energy migration is fast and that several ions display a very efficient luminescence in this host. The role of the O(1) ion has positive and negative aspects when potential applications are considered.

2. Experimental details

Samples were prepared as described in ref. 1. All preparations were performed in air, except for those cases where Tb^{3+} or Ce^{3+} was used as an activator. A slightly reducing atmosphere was then applied (N_2 with a few per cent of H_2). Unless otherwise stated, the activator concentration is 5 mol%. All samples were checked by X-ray powder diffraction and found to be single phase.

Diffuse reflection spectra were measured on a Perkin–Elmer Lambda 5 spectrometer equipped with a diffuse reflection unit. Luminescence spectra were measured on a Perkin–Elmer MPF44B spectrofluorometer. All measurements were performed at room temperature. Quantum efficiencies were estimated by comparison with standard phosphors.

3. Results and discussion

3.1. *The host lattice $Ca_4GdO(BO_3)_3$*

On excitation into the $^8S \rightarrow {}^6I$ transition of Gd^{3+} (around 273 nm) we observed a strong emission due

0925-8388/93/$6.00

to Gd^{3+} ($^6P \rightarrow {}^8S$, around 313 nm). Figure 1 shows this emission. For the same excitation wavelength we observed a weak Eu^{3+} and a weak Tb^{3+} emission (total intensity 1% or less of the overall intensity). Since our starting material Gd_2O_3 contains 10 ppm or less of impurities, this observation points to efficient energy transfer from Gd^{3+} to the impurities. Figure 2 shows the excitation spectrum of this Eu^{3+} emission. The Gd^{3+} excitation lines do indeed dominate.

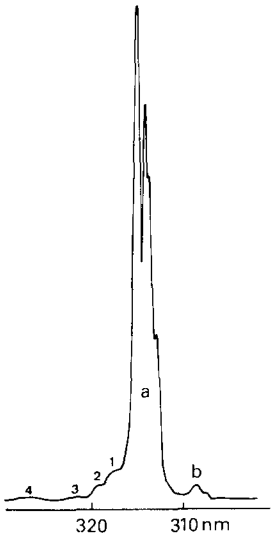

Fig. 1. The Gd^{3+} $^6P \rightarrow {}^8S$ emission of $Ca_4GdO(BO_3)_3$ under 273 nm excitation, *i.e.* in the Gd^{3+} $^8S \rightarrow {}^6I$ transition. The letters "a" and "b" indicate the electronic transitions, while the figures 1–4 indicate the vibronic transitions (see text).

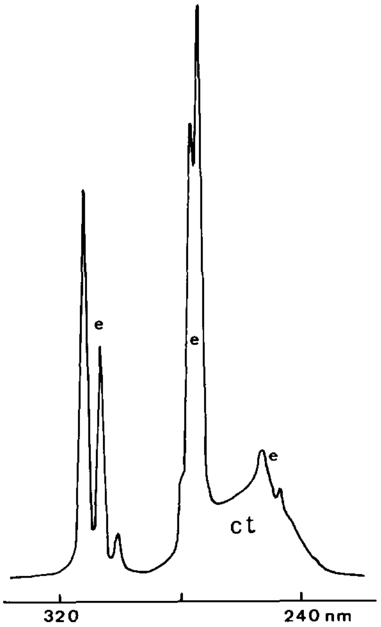

Fig. 2. The excitation spectrum of the Eu^{3+}–impurity emission of $Ca_4GdO(BO_3)_3$. The letter "e" indicates the intraconfigurational $4f^7$ transitions of Gd^{3+}, while "ct" indicates the Eu^{3+} charge transfer transition.

The Gd^{3+} emission spectrum (Fig. 1) shows two electronic transitions, namely $^6P_{7/2} \rightarrow {}^8S$ (around 314 nm) and the thermally activated $^6P_{5/2} \rightarrow {}^8S$ (around 309 nm). The former is seen to be split into four lines, as expected for C_s site symmetry. The interesting aspect is the vibronic sideband on the longer wavelength side [4]. It consists of four bands, namely two relatively strong ones at about 250 and 500 cm^{-1} from the electronic transition and two very weak ones at about 750 and 1200 cm^{-1}. The latter are due to coupling with the bending and stretching IR modes of the BO_3^{3-} group respectively; the former are due to coupling with Gd–O vibrations. Similar assignments have been given before in the case of $GdAl_3B_4O_{12}$ [5].

The striking difference between the vibronics of $Ca_4GdO(BO_3)_3$ and those of $GdAl_3B_4O_{12}$ is that those due to coupling with the borate vibrations are much weaker in the borate under study, whereas those due to coupling with the Gd–O vibrations are much stronger in $Ca_4GdO(BO_3)_3$. Actually, those of $Ca_4GdO(BO_3)_3$ show a strong similarity to those of Gd^{3+} in Y_2O_3 [6]. This observation can be understood from a consideration of the crystal structures. Whereas Gd^{3+} in $GdAl_3B_4O_{12}$ is coordinated by six oxygen ions belonging to BO_3^{3-} groups, the Gd^{3+} ion in $Ca_4GdO(BO_3)_3$ has only four of these ions and, at a shorter distance, two "free" oxygen ions (O(1)). Coupling with the latter dominates. This trend will return for other lanthanide ions.

Figure 2 shows that the emission of the Eu^{3+} impurity is excited in the Gd^{3+} levels. The weak broad band is the Eu^{3+} charge transfer band (see below). Since the Eu^{3+} concentration is only a few parts per million, one-step transfer from Gd^{3+} to Eu^{3+} is insufficient to explain the results. A considerable amount of Gd^{3+} migration must occur. The shortest Gd–Gd distance is about 3.6 Å, which is much shorter than the critical distance for Gd–Gd energy transfer (about 5 Å [3]). Therefore this migration is no surprise. In view of the crystal structure it has a one-dimensional character.

Since the Gd^{3+} energy migration will be fast, the ratio of impurity to Gd^{3+} emission intensity (about 10^{-2}) will be equal to the impurity concentration (about 10^{-5}) times the Gd^{3+}-to-impurity transfer rate (P_{tr}) divided by the Gd^{3+} radiative rate (about 200 s^{-1}). In this way P_{tr} is estimated to be 2×10^5 s^{-1}, in good agreement with values observed in comparable systems [3].

3.2. $Ca_4GdO(BO_3)_3$:Dy

The Dy^{3+} ion was used as a luminescent lanthanide ion without allowed transitions in the normal UV region. Excitation into the Gd^{3+} ion yields mainly Dy^{3+} emission. Less than 1% of the total emission intensity originates from the Gd^{3+} ion. In the Dy^{3+} excitation spectrum the Gd^{3+} excitation lines dominate, indicating efficient energy transfer from the Gd^{3+} sublattice to Dy^{3+}. These results are in agreement with expectations based on our previous work [3] and the results for undoped $Ca_4GdO(BO_3)_3$.

In the emission spectrum (Fig. 3) the yellow $^4F_{9/2} \rightarrow {}^6H_{13/2}$ Dy^{3+} emission has a higher intensity than the blue $^4F_{9/2} \rightarrow {}^6H_{15/2}$ emission. This points to a hypersensitivity effect on the former [7, 8] (see also below, Eu^{3+}).

3.3. $Ca_4GdO(BO_3)_3$:Tb

The Tb^{3+} ion was used as an activator because it shows an allowed optical transition in the UV ($4f^8 \rightarrow 4f^7 5d$). On excitation into the Gd^{3+} levels we observed less than 0.3% Gd^{3+} emission and the well-known Tb^{3+} emission, mainly from the $^5D_4$ level. Interestingly enough, a few per cent of the Tb^{3+} emission originates from the $^5D_3$ level (Tb concentration 5 mol%). In the undoped host lattice, where the Tb concentration is of the order of a few parts per million, this amount has increased to about 10%.

Usually no $^5D_3$ emission is observed at all for Tb^{3+} in borates owing to rapid non-radiative decay from the $^5D_3$ to the $^5D_4$ level [9, 10]. This in turn is due to the high vibrational frequencies of the borate group. The observation of relatively strong $^5D_3$ emission in the present oxoborate host lattice points also to a stronger coupling with the O(1) ions than to the oxygen ions belonging to the borate group.

The excitation spectrum of the Tb^{3+} emission is given in Fig. 4. It consists of the following features:

(1) the Gd^{3+} excitation lines, indicating efficient Gd^{3+}-to-Tb^{3+} energy transfer also in this case;

(2) some Tb^{3+} $4f^8$ intraconfigurational lines;

(3) a strong Tb^{3+} $4f \rightarrow 5d$ excitation band with a maximum at about 255 nm, whose shape is modified by the Gd^{3+} and Tb^{3+} excitation lines;

(4) a weak Tb^{3+} $4f \rightarrow 5d$ excitation band with a maximum at about 310 nm (under the Gd^{3+} lines), which is the $\Delta S = 1$ component of the $4f \rightarrow 5d$ transition [11].

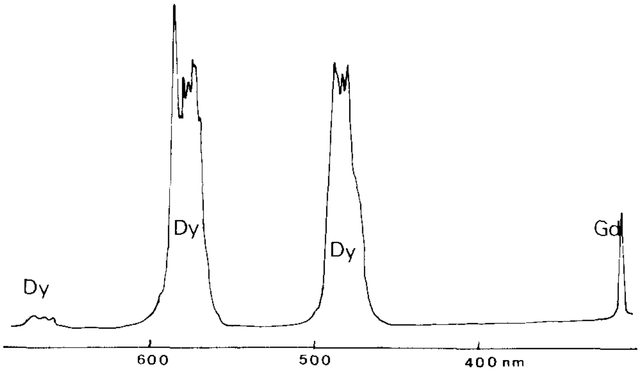

Fig. 3. The emission spectrum of $Ca_4Gd_{0.95}Dy_{0.05}O(BO_3)_3$ under Gd^{3+} excitation.

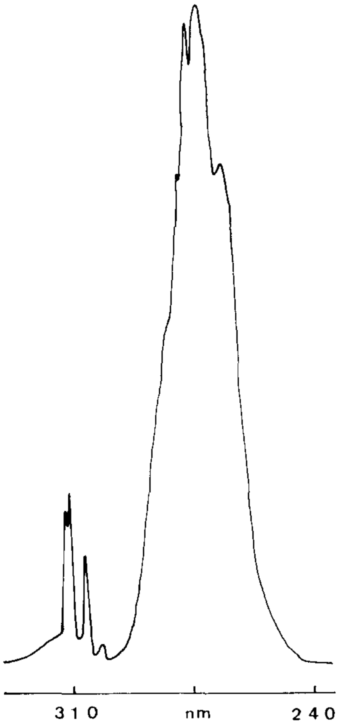

Fig. 4. The excitation spectrum of the Tb^{3+} $^5D_4$ emission of $Ca_4Gd_{0.95}Tb_{0.05}O(BO_3)_3$ (see also text). This curve is an uncorrected recorder curve (all other figures show corrected curves).

The position of the strong 4f–5d absorption band is interesting for two reasons. In the first place it makes excitation with a low pressure mercury discharge possible, so that $Ca_4GdO(BO_3)_3$:Tb is an efficient phosphor. In the second place this position is at a lower energy than that usually observed for Tb^{3+} in borates [10]. This is ascribed to the covalent influence of the O(1) ions. The same effect was reported for $SrLa_2OBeO_4$:Tb [2].

3.4. $Ca_4GdO(BO_3)_3$:Eu

The Eu^{3+} ion shows a very efficient luminescence in $Ca_4GdO(BO_3)_3$. In the emission spectrum a sharp line near 613 nm is dominant, while in the excitation spectrum a broad band with a maximum at about 260 nm dominates. The excitation spectrum shows also the Gd^{3+} excitation lines, indicating efficient energy transfer from Gd^{3+} to Eu^{3+}. The intraconfigurational $4f^6$ excitation lines of Eu^{3+} are very weak, indicating a very high quantum efficiency of the Eu^{3+} luminescence for excitation into the broad band [12]. This band is due to the charge transfer transition within the Eu^{3+}–oxygen centre and has already been mentioned above.

The position of this charge transfer band is at a relatively low energy for a borate. In $GdBO_3$:Eu^{3+}, for example, it is situated at 235 nm [13]. This is also ascribed to the covalency in the Eu–O(1) bond [2].

The $^7F_0$–$^5D_2$ excitation line of the Eu^{3+} ion at about 465 nm is known to show clearly a vibrational sideband [4, 14]. In the case of $Ca_4GdO(BO_3)_3$:Eu this sideband consists only of a vibronic band due to coupling with Eu–O vibrations. Bands due to coupling with borate vibrations could not be observed. As in the case of the Gd^{3+} ion, this indicates that the coupling with the O(1) ion is stronger than with the borate oxygens.

Part of the emission spectrum is shown in Fig. 5. The line at 613 nm dominates and has to be ascribed to the hypersensitivity of the $^5D_0$–$^7F_2$ transition involved [15]. A similar observation was made above for Dy^{3+}. The site symmetry of the rare earth ion, C_s, requires a complete splitting of the electronic lines. This is actually observed: $^5D_0$–$^7F_0$ 0, $^5D_0$–$^7F_1$ 3, $^5D_0$–$^7F_2$ 5, $^5D_0$–$^7F_3$ 7, $^5D_0$–$^7F_4$ 9. Some weak additional lines are also observed. It cannot be excluded that these indicate a small amount of site exchange between calcium and gadolinium or europium.

The composition $Ca_4EuO(BO_3)_3$ was also investigated. It shows a strong luminescence with the same characteristics as the diluted system. The quantum efficiency for excitation into the narrow Eu^{3+} lines is about six times lower for the 100% Eu sample in comparison with the 5% Eu sample. This indicates a certain amount of concentration quenching. In linear chains concentration quenching is not very effective and occurs only for concentrations above 85%. This has been investigated in $EuMgB_5O_{10}$ [16] and the present results are very similar.

Van der Voort *et al.* [12] have recently reported on the Eu^{3+} luminescence in $Ca_3(BO_3)_2$. They found two types of Eu^{3+} ions in this lattice, namely $Eu_{Ca}^{\bullet}$ and $(2Eu_{Ca}\cdot O_i)^x$. The former represents europium on a calcium site without a charge compensator in the immediate neighbourhood; the latter is an associate of two such ions and an interstitial oxygen ion. This assumption could explain the high luminescence efficiency on charge transfer excitation of the so-called associate.

A comparison of the emission spectrum of this associate (Fig. 2.b in ref. 12) with Fig. 5 shows without doubt that this emission must be due to a second phase, namely $Ca_4EuO(BO_3)_3$, which was not known at that time. It is interesting to note that although the chemical nature of the second-phase emission was derived incorrectly, the physics remains unchanged, since the O(1) ion in $Ca_4EuO(BO_3)_3$ plays a role very similar to that of the proposed interstitial oxygen ion in the associate.

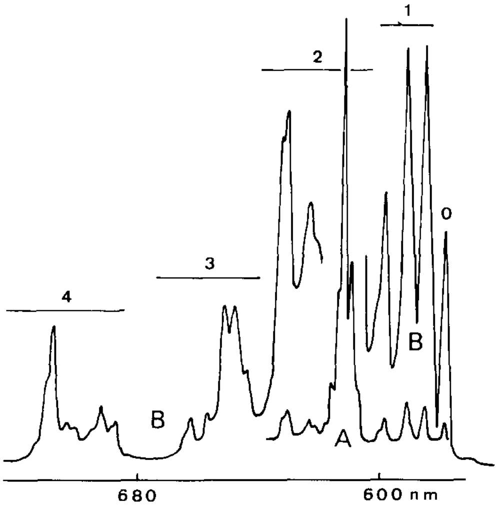

Fig. 5. The emission spectrum of the Eu^{3+} emission of $Ca_4Gd_{0.95}Eu_{0.05}O(BO_3)_3$ under Gd^{3+} and charge transfer excitation (273 nm). The figures 0–4 indicate the J value of the final level in the emission transitions $^5D_0$–^7F_J. Curve A is the full spectrum with the dominant 613 nm line. Curve B shows the weaker features (magnification about a factor of 15).

3.5. $Ca_4GdO(BO_3)_3$:Ce

The Ce^{3+} ion was used in order to study the luminescence of a lanthanide ion with broad band emission. However, the Ce^{3+} ion does not show luminescence in $Ca_4GdO(BO_3)_3$, not even at 77 K. Figure 6 gives the diffuse reflection spectrum of this composition. It has been argued before that the lowest Ce^{3+} f→d transition is at about 12 000 cm^{-1} lower energy than the corresponding f→d transition on Tb^{3+} [17]. From the value of the latter in $Ca_4GdO(BO_3)_3$, namely 255 nm (see above), we derive for Ce^{3+} a value of 370 nm. This value agrees reasonably well with the absorption onset in the diffuse reflection spectrum (Fig. 6).

The Ce^{3+} ion is known to luminesce efficiently in several borates [10, 17, 18]. The absence of luminescence

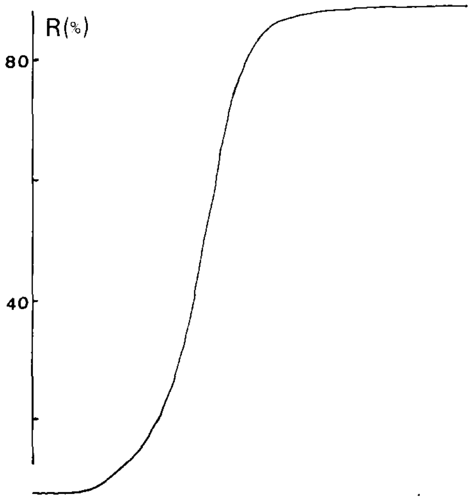

Fig. 6. The diffuse reflection spectrum of $Ca_4Gd_{0.95}Ce_{0.05}O(BO_3)_3$. R(%) is the reflection coefficient.

in $Ca_4GdO(BO_3)_3$ is therefore surprising. Also in $SrLa_2OBeO_4$ the Ce^{3+} ion did not luminesce efficiently [2]. Therefore one might think that the "free" oxygen ion has something to do with this.

The absence of Ce^{3+} emission in covalent systems has been ascribed to photo-ionization [19]. Two striking examples from that work are Y_2O_3:Ce^{3+} and La_2O_3:Ce^{3+}. Photo-ionization implies that the excited 5d level of the Ce^{3+} ion is situated close to the bottom of the conduction band.

In the crystal structure of Y_2O_3 every oxygen ion is coordinated tetrahedrally by four yttrium ions; in $Ca_4GdO(BO_3)_3$ every O(1) is also coordinated tetrahedrally by two calcium ions and two gadolinium ions, the latter forming a linear chain via O(1) with Gd–O(1)–Gd angles which are approximately equal to the tetrahedral value. Therefore we suggest that the photo-ionization involves a conduction band made up of orbitals belonging to ions in this chain. This model implies that the O(1) ions quench the luminescence of Ce^{3+}, which in borates is usually very efficient. The (absence of) luminescence of Ce^{3+} in $Ca_4GdO(BO_3)_3$ shows much more analogy with the situation in the simple lanthanide oxides than in lanthanide borates. Peculiarly enough, a similar conclusion was drawn above from the vibronic transitions in the Gd^{3+} emission spectra.

3.6. $Ca_4GdO(BO_3)_3$:Bi

The Bi^{3+} ion was investigated because it is a large trivalent ion which often luminesces efficiently. Actually, the Bi^{3+} ion shows a very efficient luminescence in $Ca_4GdO(BO_3)_3$. Figure 7 shows the luminescence spectra. There is an emission band at about 380 nm and a corresponding excitation band at 310 nm. These bands correspond to the $^1S_0 \rightleftarrows {}^3P_1$ transitions on the Bi^{3+} ion. The O(1) ion shifts this transition to a relatively low energy, since the Bi^{3+} ion in borates can usually be excited by shorter wavelengths only [10, 20]. Also, the luminescence of Bi^{3+} in $Ca_4GdO(BO_3)_3$ resembles more that in the lanthanide oxides [21] than that in borates.

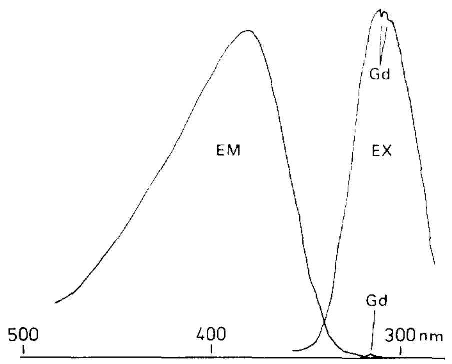

Fig. 7. Emission and excitation spectra of the luminescence of $Ca_4Gd_{0.95}Bi_{0.05}O(BO_3)_3$. Broad bands relate to Bi^{3+}, weak features indicated "Gd" relate to Gd^{3+}, EX is the excitation spectrum (for 390 nm emission) and EM is the emission spectrum (for 275 and 310 nm excitation).

Figure 7 shows very weak features due to Gd^{3+}. The emission spectrum of $Ca_4GdO(BO_3)_3$:Bi shows a very small amount of Gd^{3+} emission. This implies that a small amount of the Gd^{3+} excitation energy is not transferred to Bi^{3+}. As a consequence the excitation band of the Bi^{3+} emission shows weak dips corresponding to the $^8S \rightarrow {}^6P$ transitions of Gd^{3+}: not all the energy absorbed by Gd^{3+} reaches the Bi^{3+} ion. These features are only of minor importance, since the absorption strength of 5% Bi^{3+} is orders of magnitude larger than that of 95% Gd^{3+}.

4. Concluding remarks

(1) Several luminescent ions (Eu^{3+}, Tb^{3+}, Bi^{3+}) show a high luminescence efficiency in $Ca_4GdO(BO_3)_3$. Owing to the favourable spectral position of their broad intense excitation band, Eu^{3+} and Tb^{3+} show a high light output under 254 nm excitation. This spectral position is determined by the O(1) ions. $Ca_4GdO(BO_3)_3$:Eu^{3+} is undoubtedly a potential red lamp phosphor owing to its favourable emission spectrum and high light output.

(2) Fast energy migration occurs in the one-dimensional Gd^{3+} chains. Unfortunately, this chain cannot be sensitized by Bi^{3+} or Ce^{3+} (as in the commercial lamp phosphor $GdMgB_5O_{10}$:Ce,Tb [22]). This unfavourable effect is also due to the O(1) ions, which shift the energy levels involved to too low values.

(3) The Ce^{3+} ion does not luminesce in this borate host lattice. This is ascribed to photo-ionization.

(4) The luminescence properties of the several activators in $Ca_4GdO(BO_3)_3$ are more similar to those in the simple lanthanide oxides (*e.g.* La_2O_3, Gd_2O_3 and Y_2O_3) than to those in other borates. This becomes clear from the vibronic spectra, the rate of multiphonon decay, the hypersensitivity of certain transitions and the absence of Ce^{3+} emission. This similarity is ascribed to the strong influence of the O(1) ion in $Ca_4GdO(BO_3)_3$ on the luminescence properties. This O(1) ion is not bonded to boron and is coordinated in a similar way to the oxygen ions in the simple oxides.

References

1 R. Norrestam, M. Nygren and J. O. Bovin, *Chem. Mater.*, *4* (1992) 737.
2 G. Blasse and G. J. Dirksen, *J. Electochem. Soc.*, *136* (1989) 1550.

3 G. Blasse, *Prog. Solid State Chem., 18* (1988) 79.
4 G. Blasse, *Int. Rev. Phys. Chem., 11* (1992) 71.
5 G. Blasse and L. H. Brixner, *Eur. J. Solid State Inorg. Chem., 26* (1989) 367.
6 L. H. Brixner and G. Blasse, *J. Electrochem. Soc., 136* (1989) 3529.
7 J. L. Sommerdijk, A. Bril and F. M. J. H. Hoex-Strik, *Philips Res. Rep., 32* (1977) 149.
8 Q. Su, Z. Pei and L. Chi, in G. Adachi (ed.), *Rare Earths, Materials of the 21st Century,* The Rare Earth Society of Japan, Osaka, 1992, p. 20.
9 F. Kellendonk and G. Blasse, *J. Phys. Chem. Solids, 43* (1982) 481.
10 Hao Zhiran and G. Blasse, *Mater. Chem. Phys., 12* (1985) 257.
11 G. Blasse and A. Bril, *Philips Res. Rep., 22* (1967) 481.
12 D. van der Voort, J. M. E. de Rijk, R. van Doorn and G. Blasse, *Mater. Chem. Phys., 31* (1991) 333.
13 A. Bril and W. L. Wanmaker, *J. Electrochem. Soc., 111* (1964) 1363.
14 G. Blasse, *Inorg. Chim. Acta, 167* (1990) 33.
15 G. Blasse, in K. A. Gschneidner, Jr. and L. Eyring (eds.), *Handbook on the Physics and Chemistry of Rare Earths,* North-Holland, Amsterdam, 1979, Chap. 34.
16 M. Buys and G. Blasse, *J. Luminesc., 34* (1986) 263.
17 A. J. de Vries and G. Blasse, *Mater. Res. Bull., 21* (1986) 683; H. S. Kiliaan, F. P. van Herwijnen and G. Blasse, *Mater. Chem. Phys., 18* (1987) 351.
18 G. Blasse and A. Bril, *J. Chem. Phys., 47* (1967) 5139.
19 G. Blasse, W. J. Schipper and J. J. Hamelink, *Inorg. Chim. Acta, 189* (1991) 77.
20 H. S. Kiliaan and G. Blasse, *Mater. Chem. Phys., 18* (1987) 155.
21 G. Boulon, *J. Phys. (Paris), 32* (1971) 333.
22 M. Leskelä, M. Saakes and G. Blasse, *Mater. Res. Bull., 19* (1984) 151.